

Application of antibacterial coatings on resin composite implant materials using inkjet printing technology

Henrika Wickström¹, Annette Anthoni¹, Mirja Palo¹, Johan O Nyman¹, Anni Määttä², Mari Nurmi³, Niko Moritz⁴, Terhi Oja¹, Maren Preis¹, Niklas Sandler¹

¹Pharmaceutical Sciences Laboratory, Faculty of Science and Engineering, Åbo Akademi University, Artillerigatan 6 A, 20520 Åbo, Finland

²Laboratory of Physical Chemistry, Faculty of Science and Engineering, Åbo Akademi University, Porthansgatan 3, 20500 Åbo, Finland

³Laboratory of Paper Coating and Converting, Faculty of Science and Engineering, Åbo Akademi University, Porthansgatan 3, 20500 Åbo, Finland

⁴Turku Clinical Biomaterials Centre, Department of Biomaterials Science, University of Turku, Lemminkäinengatan 2, 20520 Åbo, Finland

Abstract

Fiber-reinforced composite (FRC) implants have shown to be a favorable option as an implant material, compared to titanium, in terms of biocompatibility and mechanical properties. Furthermore, application of antibacterial coatings onto these implant material have been presented as a viable strategy to prevent biofilm formation. The purpose of this study was to analyse the biofilm prevention effect on gentamicin coated fiber-reinforced composite implants, by means of inkjet technology, when exposed to *Staphylococcus aureus* ATCC 25923 bacteria. Scanning white light interferometry and scanning electron microscopy were used to characterize the surface texture and surface roughness of the pure and printed implant material and titanium (control) specimens. Quantification of the deposited gentamicin amount was performed using a colorimetric assay. Statistically significant biofilm inhibition was seen for the gentamicin coated resin specimens and a more than 100-fold reduction in viable cells was determined. It was concluded that piezoelectric inkjet technology could be a viable technology to precisely deposit anti-biofilm coatings onto implant materials. The presented work is based on results of a master's thesis by Anthoni et al., 2016 conducted at Åbo Akademi University [1].

Introduction

Titanium has traditionally been used as material for orthopedic implants. Different plastics and ceramics have more recently been introduced to the field. Statistics show that implant related infections are the most prevalent nosocomial complications faced in hospitals [2]. The infections are usually caused by biofilm forming bacterial strains of *Staphylococcus aureus* and *Staphylococcus epidermidis* [3]. Biofilms are formed by initial bacterial adhesion onto a surface, followed by proliferation and eventually biofilm formation. The protective extracellular matrix formed by the bacteria, makes the colonies less susceptible to the immune response of the human and also to antibiotic treatment [4].

Research has been conducted aiming to decrease the prevalence of implant related infections. Strategies in modifying the implant material by local application [5,6] or incorporation [7,8] of antimicrobial agents or by modifying the surface properties of the implant, making the implants less viable for bacteria to adhere [9], have been reported. The most recent approaches also address factors within the coating that supports bone repair [10,11].

Bone is a composite material consisting of inorganic components such as calcium phosphates, magnesium, sodium,

potassium, chlorine, iron and carbonate and organic collagens and non-collagen proteins [12,13]. Fiber-reinforced composites (FRC) have recently been introduced as an alternative implant material of low weight and with good biocompatibility [14]. Furthermore, the mechanical properties of the composites can be designed and modified [15,16].

Gentamicin is an antibiotic belonging to the aminoglycoside group, which has an antibacterial activity against both gram-positive and negative bacteria. The antibacterial activity of the drug has been reported to be concentration dependent [17]. Gentamicin has shown toxicity and drop in renal function after oral administration of 2-3 mg/kg doses [18]. However, local delivery of even higher doses of gentamicin did not result in systemic toxicity [5]. Previously, biodegradable polymeric coatings of gentamicin and poly-lactic-co-glycolic acid (PLGA) were applied onto coated stainless steel implants and controlled release of the drug was reported [6]. Application of a polymeric poly (D,L-lactide) (PDLLA) gentamicin-loaded coating on titanium wires was also shown to decrease implant-related osteomyelitis in vivo [5]. Previously, an antibacterial effect was achieved when applying coatings of silver-polysaccharide onto similar resin fiber-reinforced composites implants [19] as in the present study. Furthermore, the use of thermal inkjet printing as a coating method to deposit ink consisting of immobilized silver nanoparticles in lactose modified chitosan onto implants was proven to be a viable technique [14].

The aim of this study was to evaluate the inhibitory effect of gentamicin coatings, deposited using inkjet printing technology on FRC, for the *Staphylococcus aureus* (*S. Aureus* ATCC 25923) strain according to the static biofilm method described by Oja et al. (2014) [20]. Further aim was to investigate the surface texture of the implant after printing. The different steps of the study are visualized in Figure 1.

Materials and Methods

Preparation of implants

The implant material was prepared by mixing photopolymerizable monomers of bisphenol a glycidyl dimethacrylate (70% w/w, BisGMA) with triethyleneglycol dimethacrylate (30% w/w, TEGDMA). A photo initiator camphorquinone (0.7% w/w, CQ) and activator 2-dimethylaminoethyl methacrylate (0.7% w/w, DMAEMA) were also added to the mixture, which was stirred for 48 hours. The homogenous mixture was poured into a teflon mould and a three step photo-initiated polymerization reaction was carried out. The blocks were initially pre-cured with a dental hand

curing device for 40 sec (3M ESPE EliparTM S10), followed by 25 minutes of curing in a 95 °C light oven (Targis Power Ivoclar) and 15 minutes of post-curing in a room tempered vacuum light oven (Visio Beta Vario ESPE). The polymerized blocks were cut into pieces (7.7×7.7×1.8 mm) and polished with SiC paper grids (#2000 and #4000).

Ink preparation and printing

The broad spectrum antibiotic gentamicin sulphate salt (Sigma-Aldrich, China) was used as active pharmaceutical ingredient in this study. A gentamicin ink with a drug concentration of 15 mg/ml was prepared by dissolving the drug in a printable solvent mixture of distilled water (MQ) and propylene glycol (PG) (SAFC, Germany) (50/50-vol%). The ink was deposited onto the implants using a non-contact and drop-on-demand piezoelectric inkjet printer (PixDro LP 50, Roth & Rau, the Netherlands) and having the resolution set at 400 × 400 droplets per inch (dpi).

Viscosity and surface tension

The viscosity of solvent mixtures of MQ and PG in different ratios was measured (n = 1) using a controlled stress rheometer (Physica MCR 300 Anton Paar, Germany) equipped with a double gap measuring geometry. A shear stress range of 0.1-1000 s⁻¹ was applied at 25, 30 and 50 °C on the sample (V = 4 ml). The viscosity was determined at the highest shear rate. The surface tension (n = 3) was measured using a contact angle goniometer (CAM 200, KSV instruments) and the pendant drop method at 25 °C.

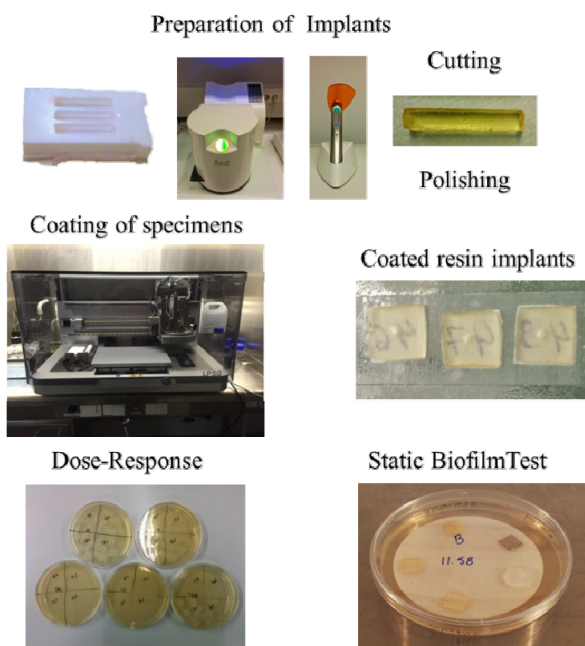


Figure 1. Pictures of the different tasks done in the study

Gentamicin quantification

Quantification of the printed gentamicin amount was performed with ultraviolet-visible (UV-Vis) spectrophotometry (Lambda 25, PerkinElmer, USA) using a validated colorimetric assay reported by Frutos et al., (2000) [21]. This assay gave rise to a purple shade due to the ninhydrin reaction of the primary and secondary amines present in the drug molecule, when right conditions were applied. An aqueous 1.25% (w/v) ninhydrin solution and a phosphate buffer (pH 7.4) were prepared

according to the method [21]. Implant specimens (n = 6) with one and two printed layers of the 15 mg/ml gentamicin ink and implants with only ink base (blank) were immersed in 1 ml of phosphate buffer (pH 7.4) for 24 hours. The ninhydrin reaction was altered as gentamicin immersed buffer solution was mixed with the ninhydrin solution (5:1.5 ratio) and put in a 95 °C pre-heated oven for 30 min (Function Line Heraeus, Thermo Fischer Scientific Inc.). The samples were cooled down on an ice bath and the absorbance was measured at 400 nm.

Biofilm inhibition

Dose-response curve

A dose-response curve of gentamicin was made to define the IC₅₀ concentration of the antibiotic against *S. aureus* ATCC 25923. The curve and the inhibitory percentage of gentamicin were performed according to the static biofilm assay described by Buckingham-Meyer et al. (2007) [22] and Oja et al. (2014) [20]. Gentamicin dilutions with different concentrations were prepared using Mueller-Hinton broth solution and pipetted onto borosilicate glass coupons (Biosurface Technologies Corporation, USA). The coupons were placed with the wetted side containing the antibiotic towards the bacterial preculture present on the Tryptic Soy Agar (TSA) plate. The TSA-plates were incubated for 24 hours at 37 °C. Biofilms formed on the coupon surfaces were collected by harvesting the coupons: the coupons were dipped in Tryptic Soy Borth (TSB), whereafter placed in a 0.5% w/v Tween-20 TSB solution and sonicated. Serial dilutions of the Tween-20 TSB solutions were made and the dilutions were plated on TSA plates and incubated for 20 hours. Colonies formed on the TSA plates were calculated and the average number of colonies, as colony forming units (CFU/ml), were determined. The data was imported in GraphPad Prism v.5.00 (GraphPad Software, USA) and IC₅₀ concentration, using 95% confidence interval, was calculated with via non-linear regression analysis, applying sigmoidal dose-response with variable slope.

Biofilm inhibition

The biofilm inhibition was studied for the resin specimens printed with one and two layers of gentamicin ink, following the static biofilm method [20]. The coated specimens were placed, with the printed side towards the filter paper, onto the plates with suspended bacteria. The plates were inoculated at 37 °C for 2, 24 or 48 hours. The 48 hour plates were moisturised after 24 hours of incubation with a 10 times diluted TSB solution. Specimens printed with one and two layers of placebo ink (solvent mixture, PG/DMSO) were used as controls. A titanium specimen, polished in the same manner as the resin specimens, was used as a control to evaluate the difference between the implant materials. The biofilms colonies were harvested as described in the section above. The colonies were calculated and data was analysed and presented as the average of log colony forming units/cm² (CFU/cm²) and % inhibition of the samples. To evaluate the statistical significance of the results unpaired, two-tailed student's t-tests were performed on the data.

Surface texture analysis

Scanning electron microscopy (SEM) and scanning white light interferometry (SWLI) measurements were performed to visualize and to characterize the surfaces of plain titanium reference specimen, plain implant surface as well as the surfaces of the resin specimens with one and two printed layers (only SWLI) of the 15 mg/ml gentamicin ink. The surface

topography characterization was done by calculation of the surface roughness (S_q , standard deviation of the height distribution of the surface) according to ISO 25178.

SWLI measurements were done using an in-house built interferometer with a NIKON 10x MIRAUI interferometry objective (NIKON IC Epi Plan DI, Japan) and a 100 μm piezoelectric z-scanner (Physik Instrumente P-721 PIFOC®, Karlsruhe, Germany). Data acquisition was done using a high-resolution CCD camera (Hamamatsu Orka Flash 2.8 CMOS, Hamamatsu City, Japan). A standard halogen lamp was used as the white light source. With this setup a final 6.3 \times magnification of the surfaces was achieved. Scanning and data acquisition was controlled with an in-house built C++ based software. 3D-image construction and 3D-data analysis (surface roughness) were performed using the commercial MountainsMap® Imaging Topography 7.2-software (Digital Surf, Avencon, France).

The scanning electron microscope used in this study (LEO Gemini 1530, Oberkochen, Germany) was equipped with a Thermo Scientific™ UltraDry™ silicon drift detector, secondary electron and backscattered electron detectors and in-lens detector. The samples were prepared by applying a thin layer of carbon coating using a vacuum evaporator. The acceleration voltage used was 5000 V, the aperture size was 30 μm and the working distance (WD) was 9 mm in every picture.

Results and Discussion

Ink formulation

In order to prepare a printable ink and to achieve a stable droplet formation, the ink needs to possess certain physical properties. The most optimal range for the inks in terms of viscosity, surface tension and density might vary depending on the printer used and on the nozzle size of the chosen print head. The measured physical properties of the ink, without gentamicin addition, are shown in Table 1.

Table 1. Physical properties of the solvent mixture

Temperature (°C)	Viscosity (mPa·s)	Surface tension (mN/m)	Density (kg/l)
25	6.5	44.0	1.04

It is important to control the temperature of the print head during the printing task, as the viscosity of the ink changes with temperature. A change might give rise to unwanted droplet formation. Due to this the viscosity was determined at the printing temperature 25 and higher temperatures of 30 and 50 °C. The viscosity values were measured to be 5.8 (30 °C) and 3.2 mPa·s (50 °C). When printing drug containing inks, unfavourable droplet formation affects the patterning and consequently the content uniformity of the drug. The printed one-layer-samples showed good content uniformity ($17.65 \pm 0.28 \mu\text{g}$, $n = 4$). The printed dose deviated slightly more ($28.30 \pm 3.89 \mu\text{g}$, $n = 3$) for the samples where two layers were printed on top of each other. The colorimetric quantification method was linear within the concentration range of 2.5 to 100 $\mu\text{g/ml}$ ($R^2 = 0.9998$). The relationship between the physical properties and the droplet formation was previously studied by Jang et al., (2009) [23]. Based on the physical properties and the nozzle diameter, the inverse of the Ohnesorge number, Z , can be calculated. The formula for calculating Z is shown in Equation 1. and is based on the nozzle diameter (α), the density (ρ), the

surface tension (γ) and the viscosity (η) of the ink. The printability range of inks was determined to be $4 \leq Z \leq 14$ [23]. In the present study the calculated Z values were 7.3, 8.3 and 14.9 for 25, 30 and 50 °C, respectively. The printing task was performed with the temperature of the print head set to 25 °C, but a slightly higher temperature (30 °C) would also have given rise to appropriate droplet ejection.

$$Z = \frac{(\alpha \rho \gamma)^{1/2}}{\eta} \quad (1.)$$

Determination of gentamicin concentration in the ink

A pre-exposure test of gentamicin against *S. Aureus* ATCC 25923 was performed in order to determine the dose-response curve and the suitability of the gentamicin concentration in the ink. The results are presented in Figure 2. According to the results a 5.41 log ng/ml gentamicin concentration would result in a 50% biofilm inhibition (IC_{50}). This value would correspond to a 2.6 μg gentamicin dose per implant specimen. A higher inhibitory effect around 90% would be achieved at concentrations of approximately 6 log ng/ml. Consequently, a dose of 10 μg of gentamicin per implant resin was determined to be optimal to determine the biofilm inhibition of the printed implants.

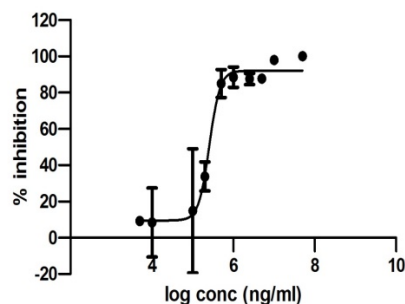


Figure 2. Dose-response curve displaying the logarithmic gentamicin concentration (ng/ml) in Mueller-Hinton broth plotted against the biofilm inhibition percentage. The points represents the mean \pm SD ($n = 23$)

Biofilm inhibition

The biofilm inhibition is presented as log CFU/cm² in Figure 3. Statistically significant biofilm inhibition was seen at 2 and 24 h for the specimens printed with one and two layers of gentamicin ink. The high inhibition percentage was explained by the printed gentamicin amounts (1 layer = $17.65 \pm 0.28 \mu\text{g}$, 2 layers = $28.30 \pm 3.89 \mu\text{g}$). A concentration of 6.4 log ng/ml seen for the one and two layer gentamicin doses correlated well with the dose-response curve of 98-99% biofilm inhibition. Inhibition percentages of 39 (1 printed layer) and 0.5 (2 printed layers) were calculated after 48 hours of incubation. A possible reason for the low inhibition percentages was due to the protocol of the static biofilm method. Moisturizing of the samples was done after 24 hours and this might have caused diffusion of antibiotic allowing the biofilms to start growing again. Since no fluid shear is present in the static biofilm test it is most optimal for simulation of biofilm formation in the ear or on the skin. However, the method was used in this study due to its simplicity and cost-effectiveness. No notable differences were detected in the biofilm inhibition between the printed placebo resins and the titanium specimens, indicating that the biofilm attachment was equal on both materials. As stated above, a 10 μg dose would have resulted in a smaller inhibition percentage, which in turn would have given more room to detect variations in the inhibitory activity of the applied

coating. According to the theoretical dose calculations the applied area (7.7×7.7 mm), the set resolution (400×400 dpi) and the chosen ink concentration (15 mg/ml) would have given rise to the intended dose of 10 µg. However, the dose calculations were based on the drop volume monitored and gained from a capture of the high-speed camera attached to the printer. These results highlight the need for proper calibration of the camera to be able to predict the printed dose.

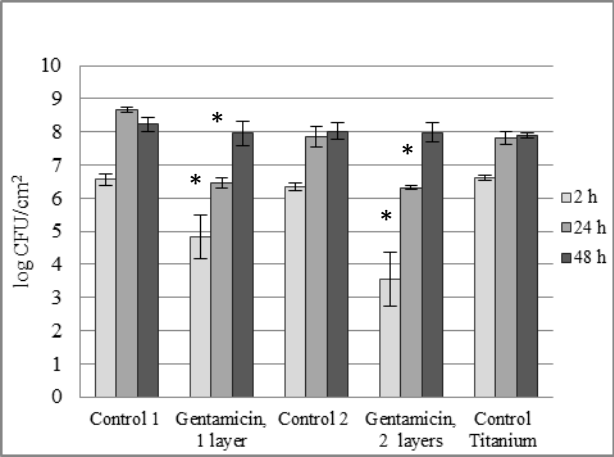


Figure 3. Anti-biofilm effect of the gentamicin coated implants, printed controls and titanium specimens. *Inhibition of statistical significance (*p*-value <0.05).

Characterization of the surface texture by SEM

Scanning electron microscopy images of polished resin specimen and a specimen with one layer of 15 mg/ml gentamicin ink are presented in Figure 4. A spatial, unaligned, droplet patterning was visualized. Due to polishing procedure and the ink properties, the spreading of the ink resulted in elongated drop patterning. After solvent evaporation and storage, dried flakes of gentamicin attached to the surface were observed (Figure 4C). The diameter of the deposited droplet after drying was 233.1 µm.

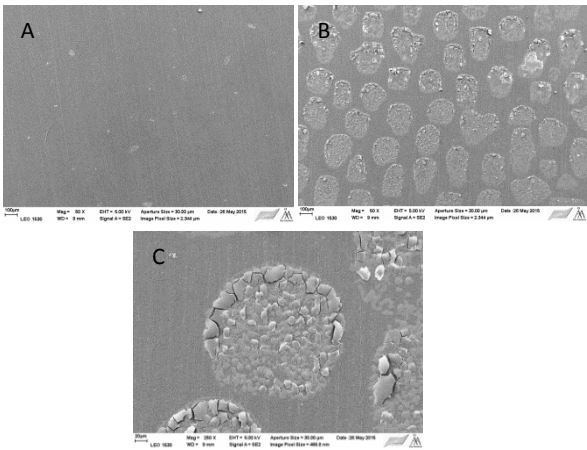


Figure 4. SEM pictures of A) a polished resin specimen (50× magnification), B) resin specimen with one layer of 15 mg/ml gentamicin ink and C) a dried droplet (250 × magnification) of the 1 layer sample

Characterization of surface roughness by SWLI

The surface textures of the different resin specimens, unprinted and printed, and of the pure titanium reference

specimen were characterized using the SWLI technique. Images obtained are presented in Figure 5.

Although same polishing treatment was applied on the titanium and the resin specimens, a clear difference in the surface roughness between the materials was determined (Table 2), 0.407 µm vs. 0.191 µm. The roughness differences were visualized in the SWLI images of these two treated materials (Figure 5A&B). Not only the roughness differed between these two surfaces, but also the topography was clearly seen to differ. Same stripes, originating from the polishing step, on the resin surface are observed in the SWLI image (Figure 5B) as in the SEM image (Figure 4A). The polished titanium surface did not show any stripe pattern, instead a random pattern originating from the polishing step was observed. In terms of biofilm formation, it has been shown that bacterial adhesion is more prevalent on rough surfaces compared to the smoother counterparts. Arnold and Bailey, (2000) [24] studied different techniques used for polishing of titanium specimens. All polished specimens showed less bacterial adhesion compared to the unpolished specimen. Furthermore, the biofilm formation was lowest for the technique resulting in the smoothest surface. Even though differences in the surface roughness were detected in this study, it did not seem to have a significant impact on the biofilm formation.

Table 2. Surface roughness (Sq) values of the studied surfaces. Roughness values of the printed samples include both printed and non-printed resin surface

Sample	Titanium specimen	Resin specimen	Resin, 1 layer	Resin, 2 layers
Sq in µm; mean±SD,n = 3	0.407 ± 0.006	0.191 ± 0.031	0.772 ± 0.224	4.150 ± 0.110

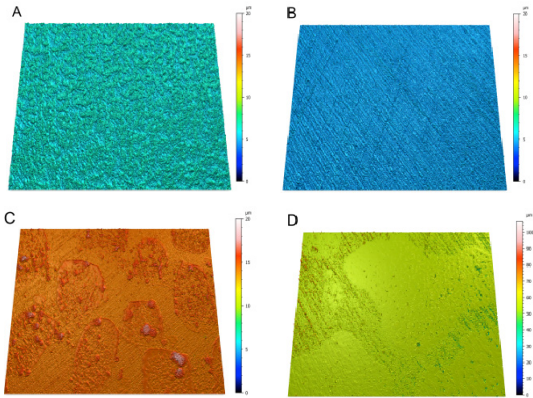


Figure 5. SWLI images of A) polished titanium surface (reference surface), B) polished resin specimen, C) resin specimen with 1 layer of 15 mg/ml gentamicin ink printed and D) resin specimen with 2 layers of 15 mg/ml gentamicin ink printed. Colour scale bar range in images A)-C) is 0-20 µm while colour scale bar range of image D) is 0-100 µm

As assumed, an increased surface roughness was detected as a means of ink deposition (Table 2). The roughness (Sq-value) was remarkably higher for the implants covered with two layers of ink compared to the roughness of both the resin reference sample and the resin with one layer gentamicin printed. The initial increase in Sq-value can be explained and is visualized in the SEM (Figure 4B) and the SWLI (Figure 5C)

images, by the flake formation, which is taking place in the printed area increasing the height deviation.

The surface roughness, as well as the ink droplet release from the printer nozzle, plays an important role when considering the ink attachment to the surface. Too low surface roughness (S_q of resin specimen = 0.191 μm) together with the ink properties are possible reasons to the observed smearing effects on the printed specimens.

Conclusions

A printable gentamicin ink formulation and fiber-reinforced composite implants were successfully prepared. A statistically significant biofilm inhibition was presented for the implants coated with gentamicin ink, showing more than a 100-fold reduction in viable cells. The biofilm growth was similar on both control specimens and the reported surface roughness difference was not seen to impact the biofilm growth on the control specimens. The ink properties and the surface roughness resulted in the elongated-drop gentamicin patterning visualized on the implant specimens. Ink deposition contributed to higher roughness values determined using SWLI. In conclusion, fiber-reinforced composite implants coated with antibacterial formulations using inkjet technology could be a potential approach in preventing implant surface infections and problems related with metal implants.

Acknowledgement

Heidi Öblom is thanked for capturing the pictures of the mould used for the implants, the PixDro printer and the static biofilm test displayed in Figure 1.

References

- [1] Annette Anthoni, Inkjet printing of antibacterial coatings on resin composite implant material, MSc thesis 2016. Åbo Akademi University, Finland
- [2] J. D. Bryers, Medical biofilms. *Biotechnology and bioengineering* 100:1-18. (2008).
- [3] Otto, Michael. "Staphylococcal biofilms." *Bacterial biofilms*. Springer Berlin Heidelberg, 2008. 207-228. [3] J. D. Bryers, Medical biofilms. *Biotechnology and bioengineering* 100:1-18. (2008).
- [4] C. R. Arciola et al. "Biofilm formation in Staphylococcus implant infections. A review of molecular mechanisms and implications for biofilm-resistant materials." *Biomaterials* 33.26 (2012): 5967-5982.
- [5] M. Lucke et al. "Gentamicin coating of metallic implants reduces implant-related osteomyelitis in rats." *Bone* 32.5 (2003): 521-531.
- [6] J. S. Price, et al. "Controlled release of antibiotics from coated orthopedic implants." *Journal of biomedical materials research* 30.3 (1996): 281-286.
- [7] H. Van de Belt et al. "Surface roughness, porosity and wettability of gentamicin-loaded bone cements and their antibiotic release." *Biomaterials* 21.19 (2000): 1981-1987.
- [8] H. Tan et al. "The use of quaternised chitosan-loaded PMMA to inhibit biofilm formation and downregulate the virulence-associated gene expression of antibiotic-resistant staphylococcus." *Biomaterials* 33.2 (2012): 365-377.
- [9] J. Fu et al. "Construction of anti-adhesive and antibacterial multilayer films via layer-by-layer assembly of heparin and chitosan." *Biomaterials* 26.33 (2005): 6684-6692.
- [10] A. Travan et al. "Polysaccharide-coated thermosets for orthopedic applications: from material characterization to in vivo tests." *Biomacromolecules* 13.5 (2012): 1564-1572.
- [11] L. Zhao et al. "Surface functionalization of titanium substrates with chitosan-lauric acid conjugate to enhance osteoblasts functions and inhibit bacteria adhesion." *Colloids and Surfaces B: Biointerfaces* 119 (2014): 115-125.
- [12] Jee WS Integrated bone tissue physiology: anatomy and physiology. In: Bone mechanics handbook, edited by Cowin SC, ISBN 0-8493-9117-2, Boca Raton, CRC Press. (2001) p. 5.1-5.13
- [13] Sara Nganga, Development of porous glass-fiber reinforced composite for bone implants-evaluation of antimicrobial effect and implant fixation. *Medica odontologica*. Painsalama Oy, Turku. (2013).
- [14] S. Nganga et al. "Inkjet printing of Chitlac-nanosilver—a method to create functional coatings for non-metallic bone implants." *Biofabrication* 6.4 (2014): 041001.
- [15] P.K. Vallittu "A Review of Fiber-Reinforced Denture Base Resins." *Journal of Prosthodontics* 5.4 (1996): 270-276.
- [16] P.K. Vallittu "Flexural properties of acrylic resin polymers reinforced with unidirectional and woven glass fibers." *The Journal of prosthetic dentistry* 81.3 (1999): 318-326.
- [17] M.K. Lacy et al. "The pharmacodynamics of aminoglycosides." *Clinical infectious diseases* 27.1 (1998): 23-27.
- [18] S.E. Cosgrove et al. "Initial low-dose gentamicin for Staphylococcus aureus bacteremia and endocarditis is nephrotoxic." *Clinical Infectious Diseases* 48.6 (2009): 713-721.
- [19] S. Nganga, et al. "In vitro antimicrobial properties of silver-polysaccharide coatings on porous fiber-reinforced composites for bone implants." *Journal of Materials Science: Materials in Medicine* 24.12 (2013): 2775-2785.
- [20] T. Oja et al. "Revisiting an agar-based plate method: What the static biofilm method can offer for biofilm research." *Journal of microbiological methods* 107 (2014): 157-160.
- [21] P. Frutos et al. "A validated quantitative colorimetric assay for gentamicin." *Journal of pharmaceutical and biomedical analysis* 21.6 (2000): 1149-1159.
- [22] K. Buckingham-Meyer et al. "Comparative evaluation of biofilm disinfectant efficacy tests." *Journal of microbiological methods* 70.2 (2007): 236-244.
- [23] D. Jang et al. "Influence of fluid physical properties on ink-jet printability." *Langmuir* 25.5 (2009): 2629-2635.
- [24] J.W. Arnold and G. W. Bailey. "Surface finishes on stainless steel reduce bacterial attachment and early biofilm formation: scanning electron and atomic force microscopy study." *Poultry science* 79.12 (2000): 1839-1845.

Author Biography

Henrika Wickström received her M.Sc. diploma from Åbo Akademi University in 2014. After her graduation she continued with her doctoral studies at the Pharmaceutical Sciences Laboratory at Åbo Akademi University and Laboratory of Pharmaceutical Process Analytical Technology at Ghent University. Her work is focused on manufacturing of printed pharmaceuticals in a flexible and continuous manner and also on analysis of the printed drug delivery systems.